Pergamon

Environment International, Vol. 22, Suppl. 1, pp. S509–S520, 1996

0160-4120/96 $15.00+.00

PII S0160-4120(96)00153-5

# EXPERIMENTAL EVALUATION OF GEOMETRICAL SHAPE FACTORS FOR SHORT CYLINDRICAL PROBES USED TO MEASURE SOIL PERMEABILITY TO AIR

R.B. Mosley
U.S. Environmental Protection Agency, National Risk Management Research Laboratory, Research Triangle Park, NC 27711, USA

R. Snoddy and S.A. Brubaker, Jr.
Acurex Environmental Corp., Research Triangle Park, NC 27709, USA

J. Brown
Dept. of Civil Engineering, North Carolina A&T State University, Greensboro, NC 27411, USA

*EI 9510-326 M (Received 18 October 1995; accepted 13 July 1996)*

Permeability of soil has become recognized as an important parameter in determining the rate of transport and entry of radon from the soil into indoor environments. This parameter is usually measured in the field by inserting a cylindrical tube with a short porous section into the soil and measuring the flow rates that result from a range of applied pressures. A variety of mathematical relationships have been used to analyze the resulting data. It is demonstrated that a commonly used mathematical approximation to describe flow through porous cylinders breaks down when the lengths of the cylinders approach their radii. It is also shown that this problem can be avoided by approximating short porous cylinders as ellipsoids. This study compared side-by-side measurements of soil permeability for a number of porous cylinders and spheres with different sizes and orientations. It is shown that all the data can be analyzed with a single curve when the appropriate shape factors (geometrical factor that describes the shape and size of the porous section of the probe) are used. This study also looked at the effects of moisture profile in the soil on the permeability obtained by different measurement methods. It is shown that the effective permeability (equivalent value for a uniform, isotropic medium) in the soil differs by two orders of magnitude in a 1-m deep soil column when the measurement locations differ by only 35 cm. The effective permeability was obtained by inverting the arithmetic average of the reciprocal values of the position-dependent permeability. 

## INTRODUCTION

Measurement of soil permeability to gases has taken on added significance in recent years as a result of increased efforts to determine entry rates of radon into buildings (Tanner 1980; Bruno 1983; Eaton and Scott 1984; Fisk et al. 1992; Garbesi et al. 1992, 1993), and to develop methods of mapping the radon potential of soils (Tanner 1986; Nazaroff et al. 1987). These efforts attempt to characterize soils in terms of their likelihood of producing elevated levels of indoor radon when buildings are constructed on them. A key component of these methods is the measurement of soil permeabilities. By far the most common type of probe used for *in situ* measurements is a small diameter tube with a short porous segment that is emplaced in the soil. The

measurements using cylindrical probes discussed in this paper refer to cylinders whose entire lengths are porous. This paper addresses two issues that arise from the interpretation of these permeability measurements. The first deals with the geometrical shape factor (a dimensionless geometrical factor times a length characteristic of the size of the active portion of the measurement probe) used to calibrate the measurement of the probe. The other issue deals with the effective permeability (equivalent value for a homogeneous, isotropic soil) of the soil and the important influence that the distributed moisture profile has on this measured value.

With regard to the geometrical shape factor for a cylindrical cavity, it has been previously shown that the usual mathematical approximations for describing the flow/pressure relationship for porous cylinders break down when the cylinders become short compared to their diameters (Mosley et al. 1994). It was demonstrated that an equivalent porous sphere makes an adequate approximation to substitute for the short porous cylinder when the length of the porous cylinder is approximately equal to its diameter. However, it is not known how well the approximation applies over a wider range of cylinder dimensions. In this paper, it will be demonstrated that an ellipsoid provides an adequate approximation for the porous section of the cylindrical permeability probes over the entire applicable range. The usefulness of ellipsoids in approximating cylinders was previously pointed out by Damkjaer and Korsbech (1992), and by van der Graaf and de Meijer (1992).

The significant influence moisture has on permeability is widely recognized. However, few people seem to take it into account adequately when measuring *in situ* permeabilities. In the EPA's large soil chamber, where the soil depth is 2 m, the moisture profile varies from nearly zero at the top surface to saturation near the bottom, where a water table is maintained. Measurements in that chamber (Mosley 1993; Mosley et al. 1993) have shown dramatic effects of the moisture profile on soil permeability. The measurements discussed in this paper were performed in a chamber that did not maintain a water table. In fact, an air plenum existed under the soil. While the variation in moisture profile is less pronounced than for the case with a water table present, its effect on permeability can still be quite significant.

## DEVELOPMENT OF EQUATIONS

Permeability is measured by emplacing a probe in the ground and measuring the relationship between an applied pressure and the resulting rate of gas flow through the probe. The applied pressure can be either positive or negative relative to the ambient. The data are analyzed based on a mathematical model for the flow/pressure relationship that properly accounts for the influence of the geometrical boundary conditions on the flow paths. The geometry of the measurement probe is important in that it determines the numerical value to be assigned to the geometrical shape factor in the mathematical model. By using a shape factor to account for the geometry of the probes, the flow/pressure relationship can be written in the same form for all probes. This so-called geometrical shape factor (van der Graaf and de Meijer 1992; Garbesi et al. 1993) really consists of the product of a dimensionless geometrical factor which depends on the shape of the probe as well as the geometry of the surrounding streamlines, and a length that is characteristic of the size of the probe. This relationship can be represented by

$$Q = S \frac{k}{\mu} \Delta P \qquad (1)$$

where,

$Q$ = volumetric flow rate ($m^3 s^{-1}$);
$S$ = geometric shape factor (m);
$k$ = permeability ($m^2$);
$\mu$ = dynamic viscosity of the gas (Pa s); and,
$\Delta P$ = applied pressure difference (Pa).

In developing models to describe the flow of soil gas through the measurement probe, it is assumed that the soil is homogeneous and isotropic in its properties that influence the movement of soil gas. Because the pressure differences to be applied are small in comparison to the ambient pressure, it is assumed that the soil gas is incompressible. As implied by Eq. 1, it is assumed that Darcy's linear relationship between flow rate and applied pressure holds, and that density variations and gravitational effects may be neglected. The other governing equation which allows a solution in the form of Eq. 1 is the continuity equation which ensures conservation of mass. Under the present assumptions, the continuity equation can be represented by Laplace's equation for the pressure field in the soil. Because of the direct analogy with the field of electrostatics, appropriate solutions to Laplace's equation for all the geometries of interest here were previously known. The shape factor for a sphere buried in a semi-infinite slab of soil was given by Nazaroff and Sextro (1989), and by van der Graaf and de Meijer (1992):

$$S = \frac{8\,p\,i\,h\,r}{2h - r} \qquad (2)$$

where,
S = shape factor (m) for the spherical cavity;
h = depth (m) of the sphere below the soil surface;
r = inner radius (m) of the spherical cavity.

Porous cylinders buried horizontal to the surface have shape factors given by Hahne and Grigull (1975):

$$S = \frac{2\pi L}{\ln\left(\frac{L}{r}\left[\sqrt{1+\left(\frac{L}{4h}\right)^2}-\frac{L}{4h}\right]\right)} \qquad (3)$$

where,
S = shape factor (m) for the porous cylinder;
L = length (m) of the cylinder;
h = depth (m) below the surface.

The shape factor for a cylinder oriented perpendicular to the surface was given by Hahne and Grigull (1975):

$$S = \frac{2\pi L}{\ln\left(\frac{L}{r}\sqrt{\frac{4h-L}{4h+L}}\right)} \qquad (4)$$

where, the symbols are the same as for Eq. 3.

The shape factor for an ellipsoid with its major axis parallel to the surface was given by van der Graaf and de Meijer (1992):

$$S = \frac{8\pi c}{\ln\left[\frac{(a+c)}{(a-c)}\frac{(\sqrt{c^2+4h^2}-c)}{(\sqrt{c^2+4h^2}+c)}\right]} \qquad (5)$$

where,
c = half the distance (m) between the foci of the ellipsoid;
a = semi-major axis (m) of the ellipsoid;
h = depth (m) below the surface.

The shape factor for an ellipsoid with its major axis perpendicular to the surface was given by Damkjaer and Korsbech (1992), and by van der Graaf and de Meijer (1992):

$$S = \frac{8\pi c}{\ln\left[\frac{(a+c)}{(a-c)}\frac{(2h-c)}{(2h+c)}\right]} \qquad (6)$$

where, the parameters are the same as for Eq. 5.

When the moisture in the soil is not distributed uniformly, the permeability, which influences the movement of soil gas, is not independent of position. Consequently, the continuity equation does not reduce to the form of Laplace's equation, but becomes

$$\nabla \cdot \frac{k}{\mu} \nabla P = 0 \qquad (7)$$

The moisture content and, consequently, the permeability vary significantly with depth in the soil. Therefore, a measurement of permeability must be interpreted in terms of an effective value of permeability. It was assumed that the soil is homogeneous and isotropic. While the mass density of the soil was measured to be uniform to within a few percent when the soil was packed into the chamber, the degree of isotropy of the flow properties of the soil is more difficult to determine. In previous studies with the same soil, an attempt was made to detect anisotropy of flow using a cubic chamber 0.3 m on an edge. Flow/pressure relationships were measured in both the vertical and the horizontal directions. No significant difference in permeability for the two transverse directions was observed. The measurements performed with this small chamber are considered preliminary and far from exhaustive in scope. While no evidence of anisotropy was observed, the soil's exposure to variations in moisture content was somewhat limited. It is possible that greater additions of pore water could result in separation of particle sizes in a manner that could lead to anisotropic effects of permeability to gas flow. For instance, smaller particles might be washed downward with a tendency to block pores at lower levels in the soil. A resulting change in local porosity could result in layers of soil having lower permeability or even having different permeabilities in the vertical and horizontal directions. Since the soil used in the current studies had been exposed to saturation

by water more than once, the possibility that some anisotropic properties were introduced can not be definitely ruled out. If some such small effects were present in the cylindrical soil chamber, they could possibly be hidden in the effective permeability measured in this study.

Consider one dimensional flow through the cylindrical chamber oriented vertically with air entering at the top soil surface and exiting into the plenum below the soil. Even though the permeability is a function of depth, Eq. 7 can be integrated twice to yield

$$\Delta P = \mu \frac{Q}{A} \int_0^L \frac{dz}{k(z)} = \mu \frac{Q}{A} \langle \frac{1}{k} \rangle L \qquad (8)$$

where, A is the cross sectional area ($m^2$) of the soil and the angle brackets indicate an average over the entire depth of the soil column. The corresponding form of Darcy's law when the permeability varies with position is

$$\Delta P = \mu \frac{Q}{A} \frac{1}{k_{eff}} L \qquad (9)$$

where, $k_{eff}$ is the effective permeability ($m^2$).

This is the value of permeability a uniform and isotropic soil would need to produce the same flow characteristics as the soil with varying permeability. Comparing Eqs. 8 and 9 shows that the effective permeability is obtained by inverting the arithmetic average of the reciprocal values of the position-dependent permeability,

$$k_{eff} = \langle \frac{1}{k} \rangle^{-1} \qquad (10)$$

Note that this result is quite different from taking the reciprocal of the average permeability. If the permeability were independent of position, the effective permeability and the arithmetic average permeability would be the same.

## MEASUREMENTS

To investigate the influence of geometrical shape factor on permeability measurements, 45 cylinders and 27 spheres were studied in a large chamber filled with sandy soil. The chamber had a diameter of 2.1 m and was filled with soil to a depth of 1.1 m. The probes were located in a horizontal plane at a depth of 0.76 m. A plenum of about 10 cm in depth was maintained under the soil. The permeability of the soil was varied by changing the moisture content. The moisture profile (top to bottom) in the soil was measured at five different locations within the chamber using a Troxler Sentry 200-AP soil moisture monitor.

The probes were constructed to minimize the pressure drop resulting from flow through the surface of the probe. About half of the spherical probes were constructed from wire mesh, while the others were plastic spheres with numerous holes. The plastic spheres did not fit the analysis curve as well as those made of wire mesh. It is believed that this is because the plastic spheres have less open area, resulting in a slight pressure drop. To avoid uncertainty introduced by pressure drop produced by flow through the measurement tubes, two separate tubes were attached to each probe. One tube was used to measure the flow rate while the other measured the static pressure in the probe. The roles of these tubes were interchanged to ensure that there was no difference in the results. The cylinders were made from commercial well screens typically used to withdraw water from the soil. The well screens are made of stainless steel that has continuously spiraling slots providing a large fraction of open area for gas entry. The dimensions of the porous cylinders are shown in Table 1, while the dimensions of the porous spheres are given in Table 2.

To illustrate effects from the full range of moisture values, three sets of moisture data were selected. The first set of data to be described represents the high moisture range. These conditions were obtained by saturating the soil with a few centimeters of water standing on the surface. The water was then allowed to drain by gravity for several days. This situation simulates the condition referred to as the field capacity of the soil. With the moisture profile remaining quite stable, flow/pressure curves were measured for all the probes. The moisture profiles were measured before and after the series of permeability measurements and were found to be unchanged. Then the effective permeability of the entire soil column was determined by measuring a flow/pressure relationship for air flowing into the top of the soil and out through the plenum at the bottom.

Table 1. Characteristics of cylindrical probes for high moisture case.

| Diameter m | Length m | Slope $mm^3\ Pa^{-1}\ s^{-1}$ | S (cylinder) m | S (ellipsoid) m |
|---|---|---|---|---|
| | | Horizontal cylinders | | |
| 0.02337 | 0.009525 | 119 | -0.2802 * | 0.08710 |
| 0.02337 | 0.02540 | 164 | 0.2078 | 0.1523 |
| 0.02337 | 0.05080 | 229 | 0.2197 | 0.2028 |
| 0.02337 | 0.07620 | 267 | 0.2588 | 0.2494 |
| 0.02337 | 0.1016 | 277 | 0.2998 | 0.2935 |
| 0.02337 | 0.1270 | 348 | 0.3404 | 0.3357 |
| 0.02337 | 0.2540 | 484 | 0.5327 | 0.5309 |
| 0.02337 | 0.4572 | 822 | 0.8168 | 0.8162 |
| 0.03327 | 0.009525 | 142 | -0.1067 * | 0.1047 |
| 0.03327 | 0.02540 | 193 | 0.3851 | 0.1774 |
| 0.03327 | 0.05080 | 248 | 0.2903 | 0.2478 |
| 0.03327 | 0.07620 | 350 | 0.3199 | 0.2970 |
| 0.03327 | 0.1016 | 436 | 0.3594 | 0.3447 |
| 0.03327 | 0.1270 | 396 | 0.4008 | 0.3900 |
| 0.03327 | 0.2540 | 565 | 0.6041 | 0.5998 |
| 0.03327 | 0.4572 | 881 | 0.9080 | 0.9064 |
| | | Vertical cylinders | | |
| 0.02337 | 0.009525 | 896 | -0.2885 * | 0.08710 |
| 0.02337 | 0.02540 | 161 | 0.2078 | 0.1523 |
| 0.02337 | 0.05080 | 205 | 0.2197 | 0.2028 |
| 0.02337 | 0.07620 | 278 | 0.2588 | 0.2494 |
| 0.02337 | 0.1016 | 313 | 0.2998 | 0.2935 |
| 0.02337 | 0.1270 | 441 | 0.3404 | 0.3357 |
| 0.02337 | 0.1524 | 269 | 0.3803 | 0.3766 |
| 0.02337 | 0.2032 | 485 | 0.4578 | 0.4552 |
| 0.02337 | 0.2540 | 508 | 0.5328 | 0.5309 |
| 0.03327 | 0.009525 | 114 | -0.1067 * | 0.1047 |
| 0.03327 | 0.02540 | 197 | 0.3848 | 0.1774 |
| 0.03327 | 0.05080 | 246 | 0.2903 | 0.2478 |
| 0.03327 | 0.07620 | 320 | 0.3199 | 0.2975 |
| 0.03327 | 0.1016 | 460 | 0.3594 | 0.3447 |
| 0.03327 | 0.1270 | 489 | 0.4008 | 0.3900 |
| 0.03327 | 0.1524 | 362 | 0.4423 | 0.4339 |
| 0.03327 | 0.2032 | 552 | 0.5242 | 0.5184 |
| 0.03327 | 0.2540 | 586 | 0.6042 | 0.5998 |

* Negative shape factors are not physically meaningful.

The second set of data to be described is called the intermediate moisture range. These moisture conditions were established by continuously drawing room air down through the soil at a flow rate of 300 $cm^3\ s^{-1}$ for 5 d. Periodic moisture profile measurements were performed. The drying effects were less pronounced near the bottom of the soil column than near the top. Another set of probe measurements and a bulk permeability measurement were performed under these moisture conditions.

The third set of data to be described is called the low moisture range. These lower moisture conditions were obtained by first continuing to flow room air down through the soil at a rate of about 1000 $cm^3\ s^{-1}$. After several days, the moisture profile ceased to change. The moisture near the bottom remained significantly higher

Table 2. Characteristics of spheres for high moisture case.

| Diameter m | S m | Average slope $mm^3\ Pa^{-1}\ s^{-1}$ |
|---|---|---|
| 0.03571 | 0.2271 | 241 |
| 0.03810 | 0.2424 | 219 |
| 0.05634 | 0.3607 | 300 |
| 0.06111 | 0.3935 | 353 |
| 0.07620 | 0.4911 | 340 |
| 0.07777 | 0.5015 | 441 |

than the rest of the soil. The direction of flow was then reversed in an effort to reduce the high moisture content near the bottom. In this case, room air flowed from the plenum up through the soil and out the top surface. Periodic moisture profiles were obtained. The drying air flow was discontinued after about 20 d of flowing at a rate of about 3000 $cm^3\ s^{-1}$. Another set of probe measurements and an effective permeability measurement were performed under these low moisture conditions.

## DISCUSSION OF RESULTS

As discussed previously, it has been demonstrated that the approximations for cylinders given in Eqs. 3 and 4 break down for short cylinders. While an effective sphere can be used as an adequate correction over a limited range in which the length of the cylinder is nearly equal to the diameter, a better approximation that spans the entire range of cylinder lengths can be obtained using ellipsoids to approximate the cylinders. The ellipsoids include the case of the sphere. Figure 1 illustrates the singularity that occurs in Eq. 3 when the ratio, L/r, is near 1. The result for Eq. 4 is similar. In fact, it can be shown that when (L/4h) << 1, Eqs. 3 and 4 are identical to within first order terms of L/4h. Within this approximation, both Eqs. 3 and 4 are represented by the single curve in Fig. 1. Since negative shape factors are not physically meaningful, Eqs. 3 and 4 should not be used when values of L/r lie to the left of the singularity illustrated in Fig. 1. The negative portion of the curve shown in Fig. 1 is intended to illustrate the range of L/r for which Eqs. 3 and 4 yield nonphysical values of shape factor. It is clear that near the singularity, the error in Eqs. 3 and 4 can be quite severe. Even for a ratio of 2, the error is about 40%. It appears the ratio should be at least 6 for the error to be less than 5%. Use of the ellipsoidal approximation (Eqs. 5 and 6 with L = 2c and r equal to the semi-minor axis) throughout the entire range will avoid the problem. However,

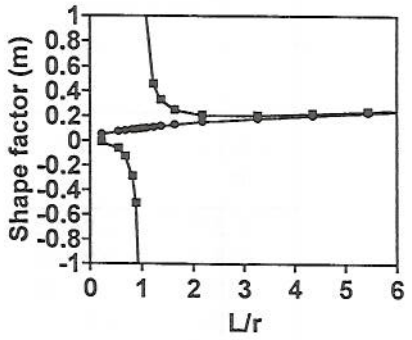


Fig. 1. Comparison of computed shape factors for a short porous cylinder (squares) and a porous ellipsoid (circles) as a function of the ratio of length to radius.

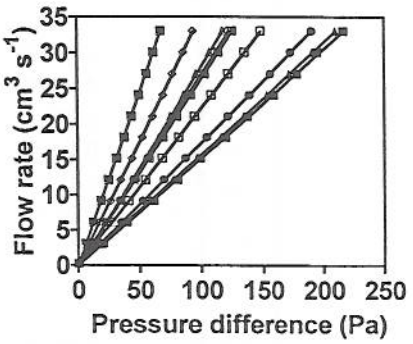


Fig. 2. A plot of the flow/pressure relationship for the nine small diameter vertical cylinders shown in Table 1.

there is also the potential for singularities in Eqs. 5 and 6 if the limit in which c approaches a is not taken properly. These singularities would occur when a = c. When a = c, the ellipsoid becomes a sphere and Eq. 2 should be used. Also a and c should be interchanged when a is less than c.

Permeability measurements associated with high moisture conditions (field capacity) will be presented first. Measurements of flow rate and pressure for nine cylinders are illustrated in Fig. 2. These are the small diameter cylinders in Table 1 that are oriented vertically. Note that the relationship is linear as expected from Eq. 1. The slopes of these curves contain both the geometric shape factor and the soil permeability (S k/μ). The permeability may be extracted by plotting the regression slopes of curves similar to the ones shown in Fig. 2 for all the probes as a function of the computed shape factors using the appropriate expressions (Eqs. 2 - 6). Since it is cumbersome to show plots for all the probes, the regression slopes from curves like those in Fig. 2 are given in Tables 1 and 2. While there were a total of 27 spheres, there were several duplicates of only six different sizes. Table 2 shows the average slope for each of the six sizes. These regression slopes are then

plotted as a function of their respective shape factors as shown in Fig. 3. Most of the outliers on the lower side of the curve correspond to the plastic spheres. Because of their low fraction of open surface area, these spheres behave as if they have smaller effective shape factors. Of course, another way to view these results is that a small pressure drop is associated with the surface of the plastic sphere, causing the corresponding regression slope to be too small. Including these outliers, however, has little effect on the slope computed by linear regression. Multiplying the regression slope from Fig. 3 by the soil gas viscosity (18.3 μPa s) yields a value of 16.9 $\mu m^2$ for the permeability. Figure 4 shows the flow/pressure relationship for the measurement of ef fective permeability. Using Eq. 9, the effective permeability can be computed from the slope of Fig. 4 as $k_{eff}$ = 0.139 $\mu m^2$, where the length of the column is 1.1 m and the diameter is 2.1 m. Note that these two measurements of permeability produce tremendously different results. They differ by a factor of 121. It's not a matter of one of these measurements being wrong. It is simply a matter of understanding what the two procedures are measuring. In the first case, the probes are located 76 cm below the surface of the soil and are primarily sampling the effective permeability along flow paths from the upper soil surface to the individual probes. These flow paths are contained in the portion of the soil that lies above the region of highest moisture content. Consequently, the effective permeability for the probe measurements is two orders of magnitude larger than the effective permeability experienced by the air that traverses the entire length of the soil column. These points are dramatically illustrated in Fig. 5, which shows both the moisture and the permeability profiles in the same figure. The measured moisture profile is denoted by the squares while the permeability is denoted by circles. The permeability profile is computed from the measured moisture using a model by Rogers and Nielson (1991) ($k = 2.7\exp(-12s^4)$, where s is the fraction of saturation). The effective permeability (0.121 $\mu m^2$) for the entire soil column computed from Eq. 10 is denoted in the figure by triangles. This result was obtained by numerically integrating the reciprocal of the permeability function shown in Fig. 5. This value of effective permeability obtained by numerical integration differs by 13% from the value obtained in Fig. 4. The shape of the permeability curve in Fig. 5 explains why the two measured permeabilities are so different. It is essentially because the effective permeability is the inverted value of the arithmetic average of the reciprocal permeability rather than the

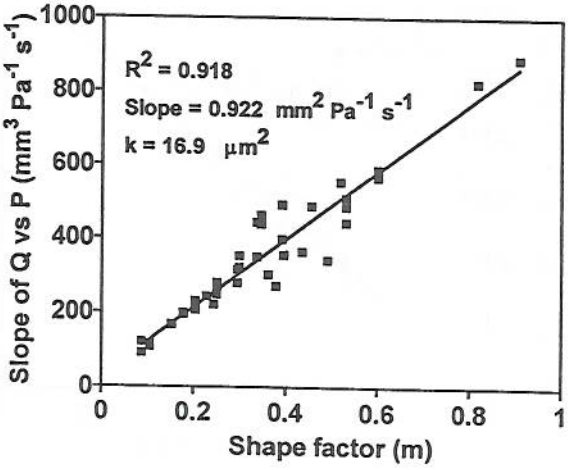


Fig. 3. A plot of the regression slopes of the flow curves as a function of shape factor for all probes with high moisture content.

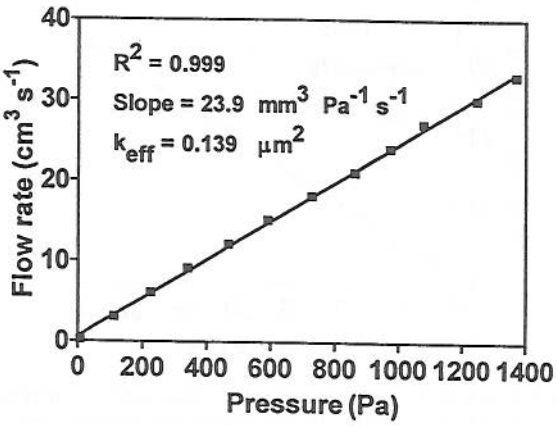


Fig. 4. A plot of the flow/pressure relationship used to determine the effective permeability for the high moisture case.

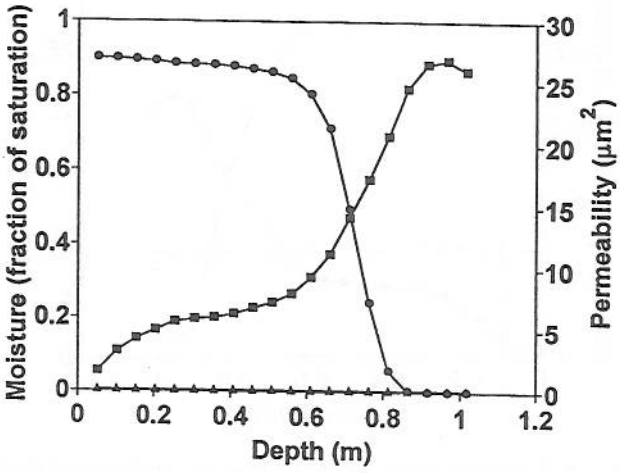


Fig. 5. A composite graph showing the moisture content (squares), the local permeability (circles), and the effective permeability (triangles) as a function of depth in the soil.

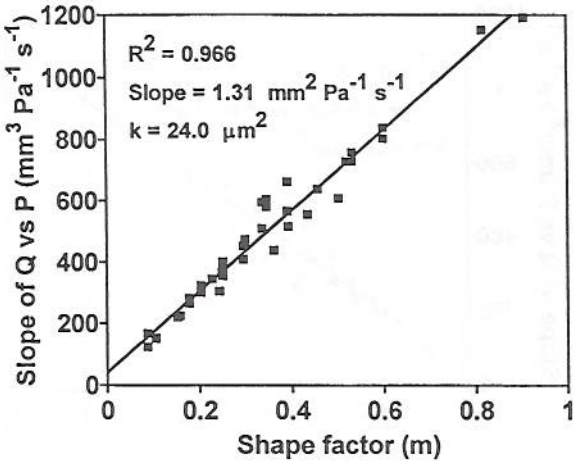


Fig. 6. A plot of the regression slopes of the flow curves as a function of shape factor for all probes with intermediate moisture content.

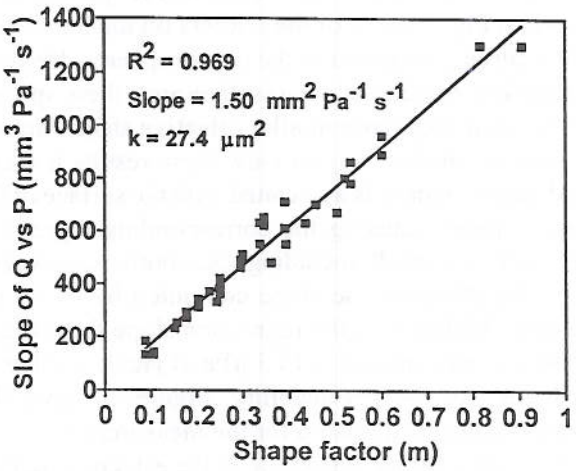


Fig. 9. A plot of the regression slope of the flow curves as a function of shape factor for all probes for the case of low moisture content.

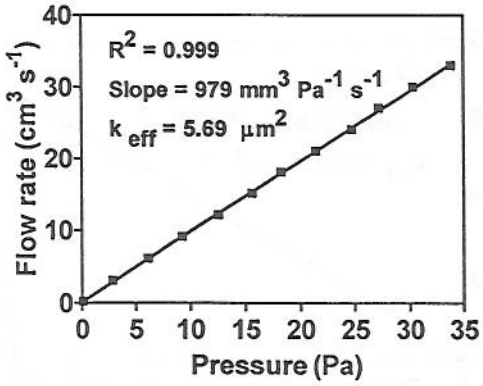


Fig. 7. A plot of the flow/pressure relationship used to determine the effective permeability for the intermediate moisture case.

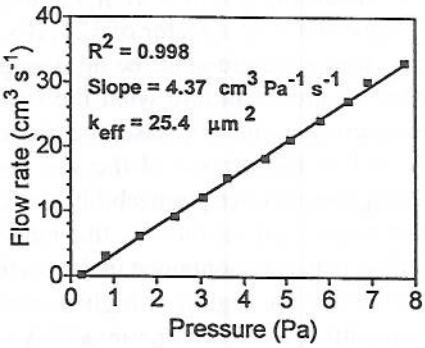


Fig. 10. A plot of the flow/pressure relationship used to determine the effective permeability for the low moisture case.

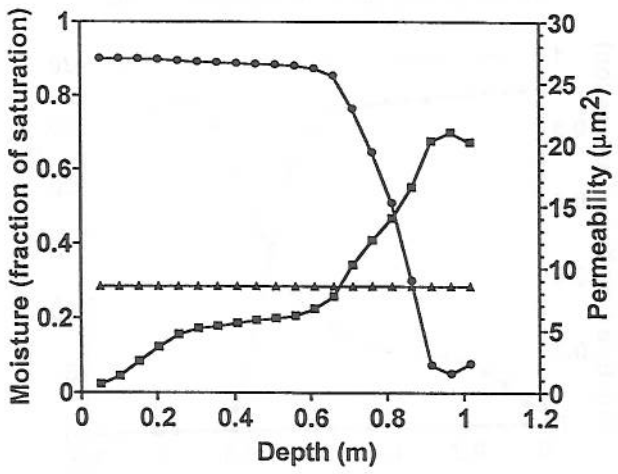


Fig. 8. A composite graph showing the moisture content (squares), the local permeability (circles), and the effective permeability (triangles) as a function of depth in the soil.

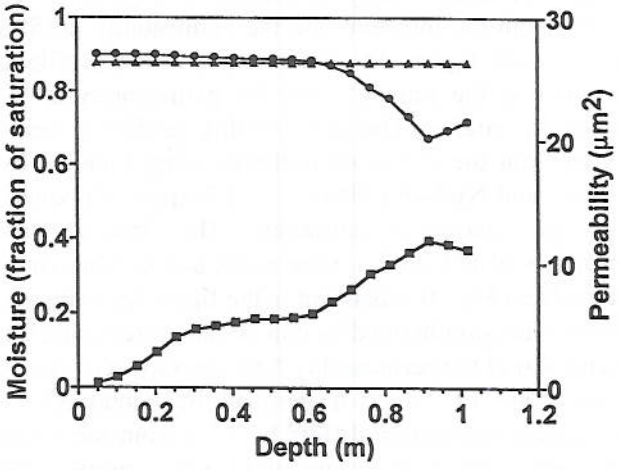


Fig. 11. A composite graph showing the moisture content (squares), the local permeability (circles), and the effective permeability (triangles) as a function of depth in the soil.

Table 3. Characteristics of cylindrical probes for intermediate moisture case.

| Diameter m | Length m | Slope $mm^3\ Pa^{-1}\ s^{-1}$ | S (cylinder) m | S (ellipsoid) m |
|---|---|---|---|---|
| Horizontal cylinders | | | | |
| 0.02337 | 0.009525 | 170 | -0.2802 * | 0.08710 |
| 0.02337 | 0.02540 | 220 | 0.2078 | 0.1523 |
| 0.02337 | 0.05080 | 321 | 0.2197 | 0.2028 |
| 0.02337 | 0.07620 | 380 | 0.2588 | 0.2494 |
| 0.02337 | 0.1016 | 410 | 0.2998 | 0.2935 |
| 0.02337 | 0.1270 | 510 | 0.3404 | 0.3357 |
| 0.02337 | 0.2540 | 730 | 0.5327 | 0.5309 |
| 0.02337 | 0.4572 | 1200 | 0.8168 | 0.8162 |
| 0.03327 | 0.009525 | 150 | -0.1067 * | 0.1047 |
| 0.03327 | 0.02540 | 260 | 0.3851 | 0.1774 |
| 0.03327 | 0.05080 | 350 | 0.2903 | 0.2478 |
| 0.03327 | 0.07620 | 470 | 0.3199 | 0.2975 |
| 0.03327 | 0.1016 | 580 | 0.3594 | 0.3447 |
| 0.03327 | 0.1270 | 560 | 0.4008 | 0.3900 |
| 0.03327 | 0.2540 | 800 | 0.6041 | 0.5998 |
| 0.03327 | 0.4572 | 1200 | 0.9080 | 0.9064 |
| Vertical cylinders | | | | |
| 0.02337 | 0.009525 | 120 | -0.2885 * | 0.08710 |
| 0.02337 | 0.02540 | 220 | 0.2078 | 0.1523 |
| 0.02337 | 0.05080 | 300 | 0.2197 | 0.2028 |
| 0.02337 | 0.07620 | 400 | 0.2588 | 0.2494 |
| 0.02337 | 0.1016 | 450 | 0.2998 | 0.2935 |
| 0.02337 | 0.1270 | 590 | 0.3404 | 0.3357 |
| 0.02337 | 0.2032 | 640 | 0.4578 | 0.4552 |
| 0.02337 | 0.2540 | 760 | 0.5328 | 0.5309 |
| 0.03327 | 0.009525 | 150 | -0.1067 * | 0.1047 |
| 0.03327 | 0.02540 | 280 | 0.3848 | 0.1774 |
| 0.03327 | 0.05080 | 360 | 0.2903 | 0.2478 |
| 0.03327 | 0.07620 | 460 | 0.3199 | 0.2975 |
| 0.03327 | 0.1016 | 600 | 0.3594 | 0.3447 |
| 0.03327 | 0.1270 | 660 | 0.4008 | 0.3900 |
| 0.03327 | 0.1524 | 550 | 0.4423 | 0.4339 |
| 0.03327 | 0.2032 | 730 | 0.5242 | 0.5184 |
| 0.03327 | 0.2540 | 840 | 0.6042 | 0.5998 |

* Negative shape factors are not physically meaningful.

arithmetic average of the permeability itself. The arithmetic average of the permeability would be heavily weighted toward the high values that the buried probes see, while the arithmetic average of the reciprocal is heavily weighted toward the low values near the bottom of the soil column. The effective value, if computed for the probe position, should also agree well with the probe measurements because the integral of the reciprocal permeability does not extend into the lower region of the soil where the lowest values of permeability exist.

Table 4. Characteristics of spheres for intermediate moisture case.

| Diameter m | S m | Average slope $mm^3\ Pa^{-1}\ s^{-1}$ |
|---|---|---|
| 0.03571 | 0.2271 | 342 |
| 0.03810 | 0.2424 | 303 |
| 0.05634 | 0.3607 | 436 |
| 0.06111 | 0.3935 | 513 |
| 0.07620 | 0.4911 | 484 |
| 0.07777 | 0.5015 | 606 |

Table 5. Characteristics of cylindrical probes for low moisture case.

| Diameter m | Length m | Slope $mm^3\ Pa^{-1}\ s^{-1}$ | S (cylinder) m | S (ellipsoid) m |
|---|---|---|---|---|
| Horizontal cylinders | | | | |
| 0.02337 | 0.009525 | 180 | -0.2802 * | 0.08710 |
| 0.02337 | 0.02540 | 250 | 0.2078 | 0.1523 |
| 0.02337 | 0.05080 | 340 | 0.2197 | 0.2028 |
| 0.02337 | 0.07620 | 390 | 0.2588 | 0.2494 |
| 0.02337 | 0.1016 | 460 | 0.2998 | 0.2935 |
| 0.02337 | 0.1270 | 550 | 0.3404 | 0.3357 |
| 0.02337 | 0.2540 | 780 | 0.5327 | 0.5309 |
| 0.02337 | 0.4572 | 130 | 0.8168 | 0.8162 |
| 0.03327 | 0.009525 | 140 | -0.1067 * | 0.1047 |
| 0.03327 | 0.02540 | 270 | 0.3851 | 0.1774 |
| 0.03327 | 0.05080 | 360 | 0.2903 | 0.2478 |
| 0.03327 | 0.07620 | 510 | 0.3199 | 0.2975 |
| 0.03327 | 0.1016 | 620 | 0.3594 | 0.3447 |
| 0.03327 | 0.1270 | 610 | 0.4008 | 0.3900 |
| 0.03327 | 0.2540 | 890 | 0.6041 | 0.5998 |
| 0.03327 | 0.4572 | 1300 | 0.9080 | 0.9064 |
| Vertical cylinders | | | | |
| 0.02337 | 0.009525 | 130 | -0.2885 * | 0.08710 |
| 0.02337 | 0.02540 | 230 | 0.2078 | 0.1523 |
| 0.02337 | 0.05080 | 310 | 0.2197 | 0.2028 |
| 0.02337 | 0.07620 | 420 | 0.2588 | 0.2494 |
| 0.02337 | 0.1016 | 490 | 0.2998 | 0.2935 |
| 0.02337 | 0.1270 | 630 | 0.3404 | 0.3357 |
| 0.02337 | 0.1524 | 490 | 0.3803 | 0.3766 |
| 0.02337 | 0.2032 | 700 | 0.4578 | 0.4552 |
| 0.02337 | 0.2540 | 860 | 0.5328 | 0.5309 |
| 0.03327 | 0.009525 | 130 | -0.1067 * | 0.1047 |
| 0.03327 | 0.02540 | 290 | 0.3848 | 0.1774 |
| 0.03327 | 0.05080 | 380 | 0.2903 | 0.2478 |
| 0.03327 | 0.07620 | 490 | 0.3199 | 0.2975 |
| 0.03327 | 0.1016 | 650 | 0.3594 | 0.3447 |
| 0.03327 | 0.1270 | 710 | 0.4008 | 0.3900 |
| 0.03327 | 0.1524 | 630 | 0.4423 | 0.4339 |
| 0.03327 | 0.2032 | 800 | 0.5242 | 0.5184 |
| 0.03327 | 0.2540 | 960 | 0.6042 | 0.5998 |

* Negative shape factors are not physically meaningful.

Table 6. Characteristics of spheres for low moisture case.

| Diameter m | S m | Average slope $mm^3\ Pa^{-1}\ s^{-1}$ |
|---|---|---|
| 0.03571 | 0.2271 | 368 |
| 0.03810 | 0.2424 | 325 |
| 0.05634 | 0.3607 | 484 |
| 0.06111 | 0.3935 | 554 |
| 0.07620 | 0.4911 | 539 |
| 0.07777 | 0.5015 | 665 |

Figures 6, 7, and 8 show a similar series of measurements for an intermediate range of moisture. Slopes of the flow curves similar to Fig. 2 are given in Tables 3 and 4. These regression slopes are plotted as a function of shape factor in Fig. 6. When the regression value of the slope in Fig. 6 is multiplied by the soil gas viscosity (18.3 μPa s), the permeability becomes 24.0 $\mu m^2$. Figure 7 plots the flow measurements through the full length of the soil column. The regression slope of Fig. 7 yields an effective permeability of 5.69 $\mu m^2$. In contrast to the high moisture case, this value differs by only a

factor of 4 from the permeability measured by the buried probes. Figure 8 shows that the permeability does not dip nearly so low near the bottom of the soil as for the high moisture case. As previously, the moisture curve is denoted by squares, the permeability by circles, and the effective permeability by triangles. In this case, the effective permeability lies intermediate between the low and high values of the permeability profile. This will typically be the case when the extreme values differ by no more than an order of magnitude.

For the low moisture case, Tables 5 and 6 contain the regression slopes obtained from curves analogous to those in Fig. 2. These slopes are plotted as a function of shape factor in Fig. 9. The slope was found by regression to be 1.50 $mm^2\ Pa^{-1}\ s^{-1}$. Multiplying the regression slope of Fig. 9 by the dynamic viscosity of the soil gas yields a permeability of 27.4 $\mu m^2$. The measured effective permeability is illustrated in Fig. 10. The slope of this curve yields a permeability of 25.4 $\mu m^2$. This effective permeability differs by only 7% from the value obtained from the buried probes. The reason for the good agreement is illustrated by the small variation in the permeability profile in Fig. 11. As before, the squares represent the moisture profile, the circles represent the permeability profile, and the triangles represent the effective permeability. Note that in this case, the effective permeability agrees more closely with the probe measurements than with the computed permeability near the bottom of the soil. Also in this case, the effective permeability computed by numerical integration differs by only 4% from the measured effective permeability.

## CONCLUSIONS

As can be seen in Tables 1, 3, and 5, horizontal and vertical orientations of the porous cylinders produce only minor differences in the calculated values of shape factor. This is true because the depth, h, used in these measurements is much larger than the cylinder length, L. A similar result occurs for the ellipsoids. This yields a simplification of the analyses and will generally be true for typical *in situ* permeability measurements. It can be concluded that Eqs. 3 and 4 are valid when the length of the cylinder is several times larger than the radius (about 10 times is the usual rule of thumb). However, these expressions break down (predict erroneous or unphysical results) when the length approaches the radius of the cylinder. Clearly, Eqs. 3 and 4 should not be used to compute the shape factor for values of L/r that are near the discontinuity illustrated in Fig. 1. Since negative values of shape factor are not physically meaningful, Eqs. 3 and 4 should never be used when the value of L/r lies to the left of the discontinuity. This does not mean that such a probe could not be used, just that Eqs. 3 and 4 should not be used to calculate the shape factor. It was illustrated that this problem can be avoided by replacing Eqs. 3 and 4 by Eqs. 5 and 6, respectively. These results also demonstrate that measurements with probes of different designs and geometry can be compared on the same curve when the appropriate shape factors are used.

Significant variation in the moisture profile can have a dramatic effect on the effective permeability that is measured at various depths in the soil. Consider the high moisture case in which the permeability measured at a depth of 110 cm was 121 times smaller than was measured at a depth of 76 cm. If the measurement in soil had been made only at the 110 cm depth, it might have been concluded that the radon potential for construction at that site was low. However, if the entry routes through the substructure of the building were located above 76 cm, there could well be a much higher entry rate of soil gas and possibly radon than would have been predicted by the permeability measurement.

## REFERENCES

Bruno, R.C. Sources of indoor radon in houses: A review. J. Air Pollut. Control Assoc. 33: 105-109; 1983.

Damkjaer, A.; Korsbech, U. A small-diameter probe for in situ measurements of gas permeability of soil. Radiat. Prot. Dosim. 45: 85-89; 1992.

Eaton, R.S.; Scott, A.G. Understanding radon transport into houses. Radiat. Prot. Dosim. 7: 251; 1984.

Fisk, W.J.; Modera, M.P.; Sextro, R.G.; Garbesi, K.; Wollenberg, H.A.; Narasimhan, T.N.; Nuzum, T.; Tsang, Y.W. Radon entry into basements: Approach, experimental structures, and instrumentation of the Small Structures Project. LBL-31864. Berkeley, CA: Lawrence Berkeley Laboratory; 1992.

Garbesi, K.; Sextro, R.G.; Nazaroff, W.W. A dynamic pressure technique for estimating permeability and anisotropy of soil to air flow over a scale of several meters. LBL-32723. Berkeley, CA: Lawrence Berkeley Laboratory; 1992.

Garbesi, K.; Sextro, R.G.; Fisk, W.J.; Modera, M.P.; Revzan, K.L. Soil-gas entry into an experimental basement: Model measurement comparison and seasonal effects. Environ. Sci. Technol. 27: 466-473; 1993.

Hahne, E.; Grigull, U. Formfaktor und Formwiderstand der stationären mehrdimensionalen Wärmeleitung (Parameter and form resistance of stationary multi-dimensional heat conductance). J. Heat Mass Transfer 18: 751-767; 1975.

Mosley, R.B. Model based pilot scale research facility for studying production, transport, and entry of radon into structures. In: Proc. 1992 international symposium on radon and radon reduction

technology. Vol. 1. EPA-600/R-93-083a. PB93-196194. Springfield, VA: National Technical Information Service; 1993: 6-123 thru 6-140.

Mosley, R.B.; Menetrez, M.Y.; Harris, D.B.; Snoddy, R.; Ratanaphruks, K.; Brubaker, S.A., Jr. Comparison of measurement techniques for soil permeability in EPA's soil-gas chamber. In: Proc. 1993 U.S. EPA/A&WMA international symposium on measurement of toxic and related air pollutants. Durham, NC. 4-7 May. Pittsburgh, PA: Air and Waste Management Association; 1993.

Mosley, R.B.; Snoddy, R.; Brubaker, S.A., Jr.; Brown, J. Comparison of soil permeability measurements using probes of different sizes and geometries. In: Proc. 1994 U.S. EPA/A & WMA international symposium on measurement of toxic and related air pollutants. Durham, NC. 3-6 May. Pittsburgh, PA: Air and Waste Management Association; 1994.

Nazaroff, W.W.; Moed, B.A.; Sextro, R.G.; Revzan, K.L.; Nero, A.V. Factors influencing soil as a source of indoor radon: A framework for geographically assessing radon source potentials. Report LBL-20645. Berkeley, CA: Lawrence Berkeley Laboratory; 1987.

Nazaroff, W.W.; Sextro, R.G. Techniques for measuring the indoor $^{222}Rn$ source potential of soil. Environ. Sci. Technol. 23: 451-458; 1989.

Rogers, V.C.; Nielson, K.K. Correlation of Florida soil-gas permeabilities with grain size, moisture, and porosity. EPA-600/8-91-039. PB91-211904. Springfield, VA: National Technical Information Service; 1991.

Tanner, A.B. Radon migration in the ground: A supplementary review. In: Gesell, T.F.; Lowder, W.M., eds. Natural radiation environment III. U.S. Department of Energy Report. V. 1. CONT-780422. Springfield, VA: National Technical Information Service; 1980: 5-56.

Tanner, A.B. Geological factors that influence radon availability. In: Proc. APCA international speciality conference - Indoor radon. Philadelphia, PA. February 1986. Publication SP-54. Pittsburgh, PA: Air and Waste Management Association; 1986: 1-12.

van der Graaf, E.R.; de Meijer, R.J. Calculation of shape factors of and pressure fields around an ellipsoidal permeability probe in some simple geometries. Tech. Doc. KVI/RV-06. Groningen, The Netherlands" Kernfysisch Versneller Instituut; 1992.